ONE MASK NICKEL MICRO-FABRICATED REED RELAY

S. Roth*, C. Marxer*, G. Feusier**, N. F. de Rooij*
*IMT, University of Neuchâtel, P.O. Box 3, CH-2007 Neuchâtel, Switzerland
**Mecanex SA, Vuarpillere 29, CH-1260 Nyon, Switzerland

ABSTRACT

This paper reports on the fabrication and experimental results of a reed relay for end-course detection application. The end-course is detected by approaching an external magnet near the device. Nickel material has been chosen for the realisation of the device because of its good magnetic properties and its ability to be electrodeposited. The fabrication process requires a single photolithography step. The relay has been fabricated using a 55 µm thick positive resist photo-patterning process developed in our laboratory. Electrical, static and dynamic characterisations have been performed. The final chip dimensions are 3 mm long, 1 mm wide and 0.4 mm thick.

INTRODUCTION

Micro-machined switches and relays have undergone an ever increasing demand over the last years. Several micro-machined relays have been presented that use electrostatic [1, 2, 3, 4], thermal [2, 5], magnetostatic [6] and electromagnetic [7] actuation.

In this paper, a one mask nickel micro-fabricated reed relay is presented. It combines high aspect ratio UV photolithography, nickel electrodeposition and copper partial etching. The working principle and the technology are also described. Electrical resistance, dynamic behaviour and process limitations has been extracted from experimental data.

WORKING PRINCIPLE AND DESIGN

Working principle

Based on the reed relay working principle, the proposed micro-relay consists of a nickel beam moving laterally, actuated by an external magnetic field, to contact an electrical connector (Figure 1). Profiled structures have been integrated in the design to concentrate the magnetic field and to insure the generation of a sufficiently large magnetic force to connect the beam. The electrical ports have been separated by an air gap from the profiled structures to avoid current leakage. It is also planed to mount a hybrid coil close to the device that can be used as a self-test function. The device will then consist of four electrical ports: the input port, the output port and two ports for the self-test coil.

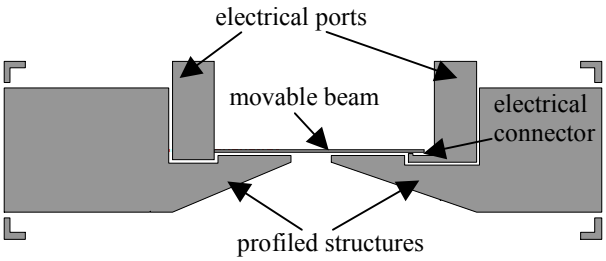

Figure 1: Schematic top view of the nickel reed relay for end-course detection application.

Design

To insure the device a good sensitivity, different parameters, such as the beam lateral spring constant and the beam/connector gap, have been considered. The beam lateral spring constant mainly depends on its length and width. The mechanical force required to close the relay is dependent on the beam spring constant and also on the beam/connector gap size. To minimise the required magnetic field needed to close the relay, the best design should have the smallest possible beam/connector gap and the largest possible length/width ratio.

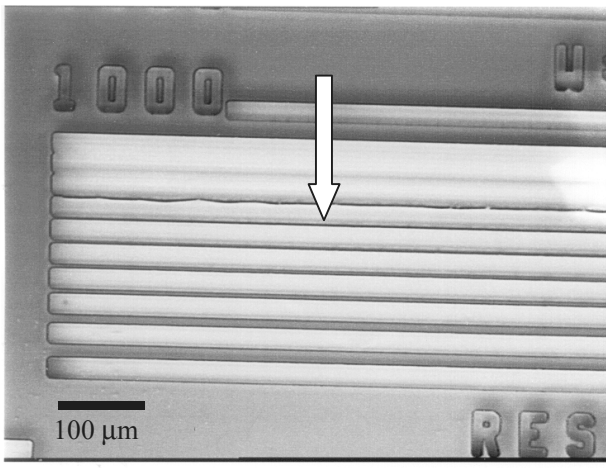

Figure 2: Microphotograph of a 55 µm thick photoresist test structure showing the minimal possible photoresist wall width of 7 µm visualised by the white arrow.

Limitations

Limitations induced by the technology have been integrated in the final design of the switch. Figure 2 shows a 55 µm thick photoresist test structure after UV photolithography and development, used to determine the minimal possible photoresist wall width. The white arrow on Figure 2 indicates that the minimal resist wall width is 7 µm (on mask), which corresponds to the minimal beam/connector gap. The minimal beam width, corresponding to the minimal resist opening, is 5 µm (on mask) [8]. No limitation has been noticed for the beam's length.

Final design

Considering the process induced limitations, relays having a 8 µm wide beam with a length of 1000 µm, 1500 µm or 2000 µm and a 10 µm beam/connector gap have been designed. A relay with a special electrical connector geometry used to reduce the lateral sticking has also been designed (Figure 3).

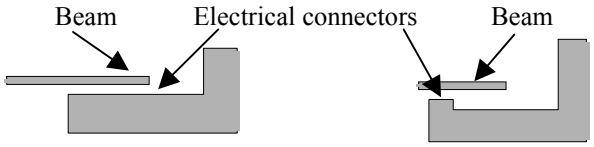

Figure 3: Schematic view of the connectors shapes: on the left the standard geometry and on the right the special geometry for sticking minimisation.

FABRICATION PROCESS

A silicon dioxide layer has been thermally grown and a silicon nitride layer has been deposited on a 4 inches silicon wafer to improve the electrical insulation. A sacrificial n-type doped silicon dioxide layer is deposited on the nitride layer, followed by the evaporation of a titanium/copper seed and sacrificial layer.

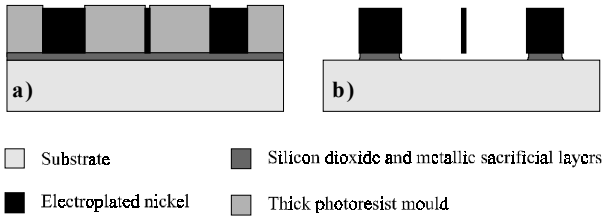

Figure 4: Schematic view of the relay fabrication process: a) Deposition of the insulating and sacrificial layers, photo-patterning of the thick resist moulds and nickel electro-deposition. b) Dissolution of the moulds and partial etching of the sacrificial layers.

To fabricate 55 µm thick photoresist moulds (Clariant AZ 4562), a 8 µm thick resist layer is first spun on the wafer and followed by the spinning of a thick resist layer as described in [8]. The total thickness is larger than expected as the first resist layer acts as an intermediate adhesive layer used to promote and to increase the second resist layer thickness.

A 95 minutes pre-bake is performed on a hot-plate at 90°. The exposure is performed with a standard UV mask aligner. Development is carried out in a Clariant AZ 400K developer solution (one part of the purchased developer diluted with four parts of de-ionised water). No post-bake is performed after development to avoid deformation of the moulds [9]. Nickel is then electrodeposited from a commercial bath (Figure 4a).

After the completed growth of the nickel layer (40 µm), the photoresist moulds are dissolved in acetone. The sacrificial layers are then partially etched to free the movable beam. The copper layer is etched in a solution of sodium peroxodisulfate and the titanium and the n-type-doped silicon dioxide layers are partially etched in buffered HF (Figure 4b). The last steps of the process consist in wafer dicing, packaging and wire bonding of the chips.

RESULTS

Technology

An increase of 3 µm (per edge) between the mask patterns and the final processed structures has been measured. The final beam width and beam/connector gap have dimension of 14 µm and 4 µm respectively compared to the 8 µm and 10 µm, respectively, designed on the mask. Figure 5 shows the 40 µm thick nickel relay after dicing.

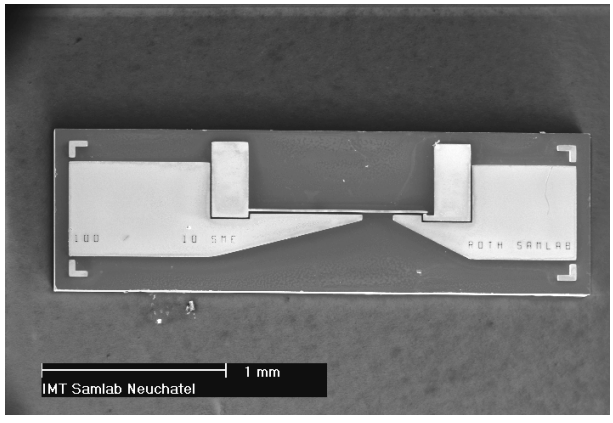

Figure 5: SEM picture of a nickel reed relay used for end-course detection application. Chip dimensions are 1 x 3 x 0.4 mm^3.

Figure 6 shows a detail of the beam/connector contact area. The shape of the connector was chosen to reduce the risk of sticking between the beam and the connector.

Figure 7 shows the fabricated device integrated into a Surface Mounted Device (SMD) package. The next generation of the relay will include a coil mounted close to the device that will be used for its self-testing.

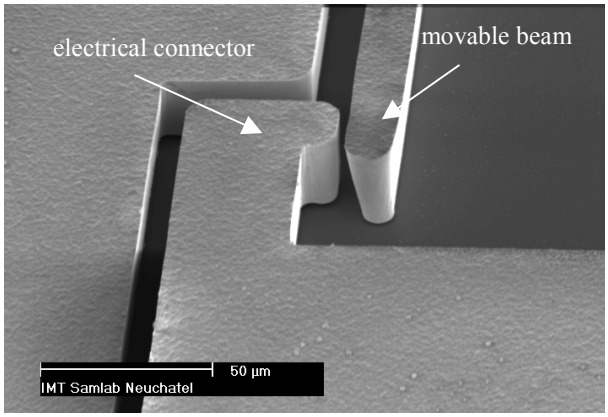

Figure 6: SEM picture of the beam/connector. Gap width is approximately 4 µm. The movable beam is 1 mm long, 14 µm wide and 40 µm thick.

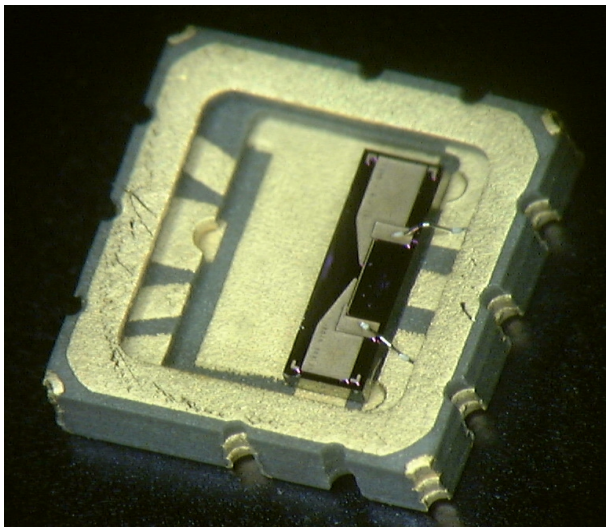

Figure 7: Picture of the relay wire-bonded on the SMD package. In the future generation, a coil will be mounted near the device.

Electrical resistance

Electrical resistance values have been obtained by closing the relay with an external permanent magnet (0.3 T, Figure 8) by and measuring the current-voltage curve. Table 1 shows the electrical resistance value for different switch configurations. The beams have the same width (14 µm) and the same beam/connector gap (4 µm). The electrical resistance of the relays with three different beam lengths and the resistance of the relays with the special geometry to avoid sticking have been measured. In order to improve the contact resistance, silver and gold have been deposited on nickel. The gold layer was deposited with an electroless process and the silver layer was evaporated.
For potentials up to 100 Volts, the electrical resistance of an open relay has been measured bigger than 1 G Ω.

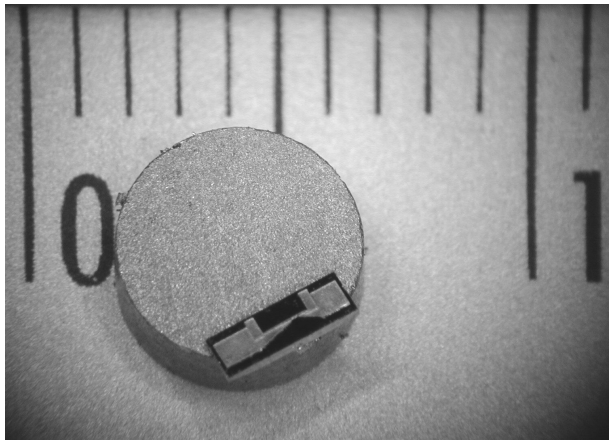

Figure 8: Picture of the relay and the permanent magnet used to close it.

Discussion

The beam length seems to have no effect on the electrical resistance, but it strongly determines the position of the magnet needed to close the switch. Shorter is the beam, larger is the force needed and closer the magnet should be. The relay with the special shape has a small beam/connector contact area, which explains its higher resistance. A surprising result is the higher resistance values measured for relays recovered by silver or gold. Further investigations are made in order to gain understanding of this phenomenon. It can be observed on Figure 6, that the slopes of the beam and of the connector are not perfectly vertical. This induces that the beam is not totally in contact with the connector. In the future, a better mould verticality should be reached to improve the contact resistance.

Table 1: Summary of the electrical resistance of the different switch configurations and contact layers.

Beam length	Gold	Silver	Nickel
1000 µm	8 Ω	10 Ω	2 Ω
1500 µm	9 Ω	11 Ω	2 Ω
2000 µm	8 Ω	10 Ω	2 Ω
1000 µm special shape	13 Ω	14 Ω	3 Ω

Dynamic measurements

The frequency behaviour of the relay has also been investigated showing that it could also be used in a dynamic mode. A coil located outside the SMD package

supplies the required oscillating magnetic field. Figure 9 shows the response of the device to an excitation signal oscillating at 10 Hz. The noise appearing during the device open phase is due to the electrical network 50 Hz interference.

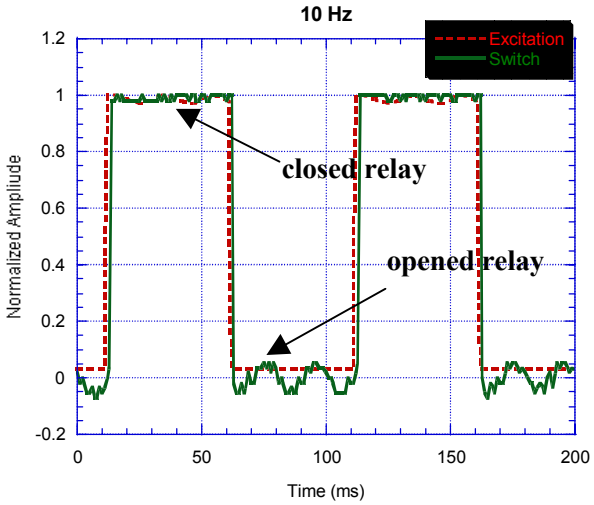

Figure 9: Response of the switch to a square magnetic field at 10 Hz as function of time.

Figure 10 shows a delay of 1.5 milliseconds of the switch driven at 100 Hz. This delay is certainly caused by the coil/relay inertia. The relay has successfully been driven up to 1 kHz (Figure 11). At this frequency the coil/relay system generates a switch closing delay of 0.5 milliseconds and a switch opening delay of 0.5 milliseconds.

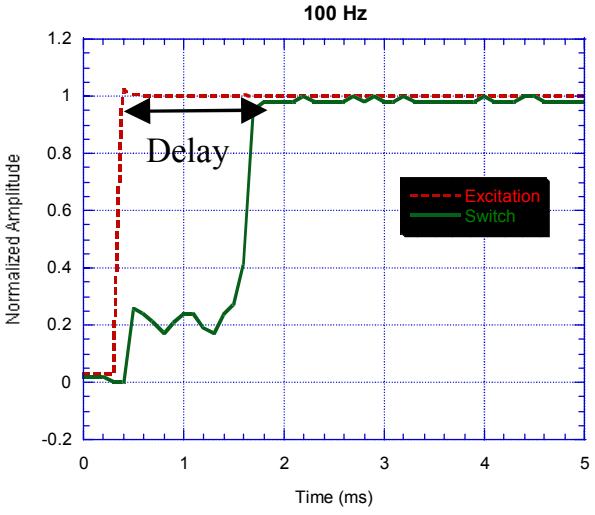

Figure 10: Close view of the rising edge of a square excitation at 100 Hz. At this frequency, the coil/relay system generates a delay of about 1.5 milliseconds.

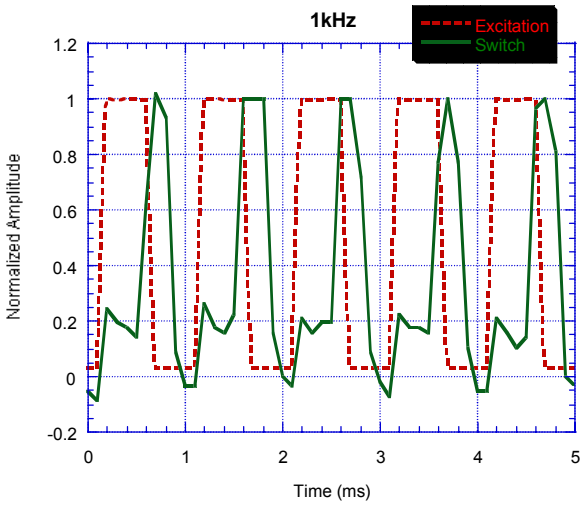

Figure 11: Device response to a 1 kHz square signal. External coil inertia limits the relay responding time.

CONCLUSION

In this paper we have shown the possibility to fabricate a nickel reed relay for end-course detection application with a single photolithography step process. We demonstrate the possibility to use the device for static and also dynamic detection. Static functionality has been demonstrated with a commercial magnet. A closed-relay electrical resistance of 2 Ω has been measured and an opened-relay electrical resistance higher than 1 GΩ has also been measured. The dynamic working range of the device has been tested with an external coil and measurements up to 1 kHz have successfully been performed. The external excitation system has to be improved to obtain a higher frequency working range. In the future, the integration of a self-test coil into the SMD package will be investigated.

ACKNOWLEDGEMENTS

This project is founded by the European Space Agency. The authors would like to thank P.-A. Clerc for the nickel electrodeposition, G. Mondin for the depositions of the different layers, S. Pochon for the dicing, the packaging and the wire bonding and Dr. A. Daridon for reading this paper.

REFERENCES

[1] M.-A. Grétillat, F. Grétilllat and N. F. de Rooij, “Micromechanical relay with electrostatic actuation and metallic contacts”, Technical Digest Tranducers ’99, pp. 1280-1283, Sendai, Japan.

[2] S. Zhou, X. Q. Sun and W. N. Carr, “A monolithic variable inductor network using microrelays with combined thermal and electrostatic actuation”, J. Micromech. Microeng. , 9 (1999), pp. 45-50.

[3] S. Majumder, N. E. McGruer, P. M. Zavracky, G. G. Adams, R. H Morrison, j. Krim, “Measurements and modelling of surface micromachined electrostatically actuated microswitches, Technical Digest Transducers ’97, pp. 1145-1148, Chicago, USA.

[4] M. Sakata, Y Komura, T. Seki, K. Kobayashi, K. Sano, S. Horiike, “Micromachined relay which utilises single crystal silicon electrostatic actuator”, Proc. MEMS 99, pp. 21-24, Orlando, USA.

[5] X. Q. Sun, K. R. Farmer and W. N. Carr, “A bistable microrelay based on two-segment multimorph cantilever actuators”, Proc. MEMS 98, pp. 154-159, Heidelberg, Germany.

[6] J. A. Wright and Y. C. Tai, “Magnetostatic MEMS relays for the miniaturisation of brushless DC motor controllers”, Proc. MEMS 99, pp. 594-599, Orlando, USA.

[7] H. A. C. Tilmans, E. Fullin, H. Ziad, M. D. J. Van de Peer, J. Kesters, E. Van Geffen, J. Bergqvist, M. Pantus, E. Beyne, K. Baert and F. Naso, “A fully-packaged electromagnetic microrelay”, Proc. MEMS 99, pp. 25-30, Orlando, USA.

[8] S. Roth, L. Dellmann, G.-A. Racine and N. F. de Rooij, “ High aspect ratio UV photolithography for electroplated structures”, J. Micromech. Microeng., 9 (1999), pp. 105-108.

[9] H. Miyajima and M. Mehregany, “ High-aspect-ratio photolithography for MEMS applications”, J. of Micromechanical Systems, Vol. 4, No. 4, 1995, pp. 220-229.